Towards subunit-specific proteasome inhibitors: synthesis and evaluation of peptide α′,β′-epoxyketones

Mikael Elofsson[1,*], Ute Splittgerber[1], Jayhyuk Myung[1], Royce Mohan[1] and Craig M Crews[1,2]

Background: The proteasome is a large multicatalytic protease complex (700 kDa) involved in a number of highly regulated processes. It has three major catalytic activities: a chymotrypsin-like activity, a trypsin-like activity and a post-glutamyl peptide hydrolyzing (PGPH) activity. To be useful as molecular probes, which could help dissect the cellular functions of the proteasome, inhibitors should be specific for the proteasome, active *in vivo* and selectively block only one of the three catalytic activities. To date, few inhibitors fulfill these requirements so we set out to make novel proteasome inhibitors that incorporate these characteristics.

Results: A panel of amino-terminally acetylated peptide α′,β′-epoxyketones with leucine in P1 and various aliphatic or aromatic amino acids in P2–P4 were prepared and evaluated. Most compounds selectively inhibited the chymotrypsin-like activity, while only weakly inhibiting the trypsin-like and PGPH activities. After optimization, one inhibitor, Ac-hFLFL-epoxide, was found to be more potent and selective for the inhibition of the chymotrypsin-like activity than several previously described inhibitors. This inhibitor also exhibited strong *in vivo* anti-inflammatory activity.

Conclusions: Optimization of amino-terminally acetylated peptide α′,β′-epoxyketones furnished a potent proteasome inhibitor, Ac-hFLFL-epoxide, that has an excellent selectivity for the chymotrypsin-like activity. The inhibitor also proved to be a potent antiproliferative and anti-inflammatory agent. The strong *in vivo* and *in vitro* activities suggest that this class of proteasome inhibitors could be both molecular probes and therapeutic agents.

Addresses: [1]Departments of Molecular, Cellular and Developmental Biology and [2]Department of Pharmacology, Yale University, 219 Prospect Street, New Haven, CT 06520-8103, USA.

*Present address: Organic Chemistry, Department of Chemistry, Umeå University, SE-90187 Umeå, Sweden.

Correspondence: Craig M Crews
E-mail: craig.crews@yale.edu

Key words: epoxyketone, inhibitor, proteasome, subunit specificity

Received: 27 July 1999
Revisions requested: 10 August 1999
Revisions received: 16 August 1999
Accepted: 17 August 1999

Published: 15 October 1999

Chemistry & Biology November 1999, 6:811–822

1074-5521/99/$ – see front matter

Introduction

Eukaryotic cells contain substantial amounts of a large proteolytic complex called the proteasome, which is widely recognized as the central proteolytic machinery required for nonlysosomal ubiquitin-dependent protein degradation [1]. General housekeeping functions of the proteasome include removal of improperly assembled or misfolded proteins formed as a result of mutation, heat or oxidative stress [2]. The proteasome is also responsible for protein degradation in highly regulated processes including cell-cycle progression [3], inflammatory responses, such as NF-κB activation [4], and antigen processing [5].

The catalytic core of the proteasome of eukaryotic cells comprises the 20S cylindrical part, consisting of 28 subunits forming four stacked rings [6,7]. The two central rings each contain three catalytically active β subunits that hydrolyze their substrates by a unique mode of action [6–8]. During assembly of the proteasome, cleavage of amino-terminal prosequences liberates amino-terminal threonines whose hydroxyl groups act as nucleophiles in the catalytic step. The two outer rings are noncatalytic and the seven α subunits in each ring serve as an anchor for the 19S (PA700) or 11S (PA28) regulatory particles [9,10] that cap each end to form the fully assembled proteasome. Higher vertebrates can express a γ-interferon-inducible immuno-proteasome, in which the β subunits X, Y and Z are replaced by LMP7, LMP2 and MECL1, respectively. This substitution results in altered proteolytic activities producing peptides with sequence motifs suitable for binding by MHC class I molecules [5]. The multiple catalytic subunits of the 20S proteasome exhibit three major activities: a chymotrypsin-like activity that cleaves substrates after large hydrophobic residues, a trypsin-like activity that hydrolyzes bonds after basic amino acids, and a post-glutamyl peptide hydrolyzing (PGPH) activity that cleaves after acidic residues [11]. Two less well-characterized catalytic activities have also been ascribed to the proteasome: BrAAP, which cleaves after branched-chain amino acids, and SNAAP, which cleaves after small neutral amino acids [11].

Proteasome inhibitors are valuable tools that enable the elucidation of details in cellular events regulated by the

proteasome [12]. In addition, inhibitors have potential therapeutic applications and use in mechanistic studies of the proteolytic machinery of the proteasome [12–14]. To date, several classes of proteasome inhibitors, for example the natural product lactacystin [15], peptide aldehydes [16–19], peptide α′,β′-epoxyketones [20–23], peptide glyoxals (α-keto aldehydes) [24], peptide vinyl sulfones [18,25,26] and peptide boronic acids [16,18], have been described. For an inhibitor to be useful as a molecular probe or therapeutic agent it should preferably be both potent and selective for inhibition of the proteasome. Furthermore, for use in cell culture or animal model studies, properties such as cell-membrane permeability and bioavailability should be considered. Although peptide aldehydes, which reversibly and covalently inhibit the proteasome, are among the most well-studied compounds so far, they also inhibit other proteases such as cathepsins and calpains [1,17]. This lack of specificity also holds true for peptide vinyl sulfones, which covalently inactivate both the proteasome [26] and intracellular cysteine proteases such as cathepsins and calpains [26,27]. The active form of lactacystin, *clasto*-lactacystin β-lactone, is also known to inhibit cathepsin A [28] and tripeptidyl peptidase II [29], in addition to the three catalytic activities of the proteasome [30]. Peptide boronic acids, a promising class of covalently inactivating and reversible proteasome inhibitors, show high selectivity for the proteasome over other proteases [16]. Recently bifunctional inhibitors, homodimeric or heterodimeric peptide aldehydes and maleimide-containing peptide aldehydes with improved potency and subunit selectivity have been described [31,32]. Although they are useful for *in vitro* investigations of the proteasome, their potential in cell-based systems might be limited.

Figure 1

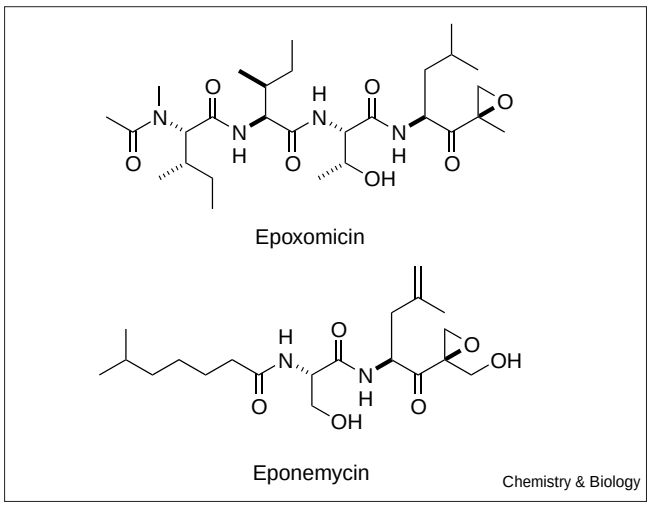

Structure of epoxomicin and eponemycin, two antitumor natural products that potently inhibit the proteasome.

Recent efforts in our lab have centered on the identification of the cellular targets of the microbial antitumor natural products epoxomicin [33] and eponemycin [34] (Figure 1). Biotinylated derivatives of epoxomicin [21] and dihydroeponemycin [35] (dihydroeponemycin retains the biological activity of eponemycin) were found to bind covalently and irreversibly to catalytic subunits of the proteasome [22,23]. Epoxomicin was found to bind X, LMP7, Z and MECL1 [22], whereas dihydroeponemycin showed selectivity for LMP2, X and LMP7 [23]. Moreover, epoxomicin is highly selective for the proteasome, and causes cell morphology change and growth arrest, leading to apoptosis [22]. In addition to the previously described antitumor activity, epoxomicin also exhibits anti-inflammatory activity in mice, presumably by inhibition of NF-kB activation [22]. Peptide α′,β′-epoxyketones [20–23] are emerging as an important class of inhibitors with promise both as molecular probes and therapeutic agents.

Our ongoing efforts are aimed at the design and synthesis of novel, more potent inhibitors with improved *in vivo* activity. Moreover, the ultimate goal is to develop inhibitors selective for each of the three major proteolytic activities of the proteasome. The use of subunit-specific inhibitors that covalently and irreversibly bind to the active sites would result in 'chemical knock-outs', which would allow the dissection of the proteasome function using a chemical genetics approach [36].

In this report we describe the synthesis of a series of peptide α′,β′-epoxyketones of varied length and amino acid sequence. These compounds were characterized for their ability to inhibit proteasomal enzymatic activity and cell growth. Furthermore, one inhibitor, which was optimized for inhibition of the chymotrypsin-like activity, exhibited strong anti-inflammatory activity *in vivo*.

Results and discussion

Design and synthesis of peptide α′,β′-epoxyketones

Catalytic subunits of the 20S proteasome accommodate various sidechains of the peptide substrate within multiple pockets on both sides of the scissile amide bond, as shown schematically in Figure 2. In addition to the key role that the P1 residue plays in subunit binding and hydrolysis, the overall length and substrate sequence contribute to defining the cleavage rate and pattern. In an analogous manner, length and sequence of inhibitors also strongly influence potency and selectivity for the three major catalytic activities of the proteasome. Inhibitors that have hydrophobic residues such as leucine and phenylalanine in P1 generally show high selectivity for the chymotrypsin-like activity [16,22,24,25,31], whereas basic residues such as lysine and arginine favour the inhibition of the trypsin-like activity [31]. Recent reports, however, indicate that variation in length and of residues in P2–P4 of inhibitors with a hydrophobic sidechain in P1 can affect

Figure 2

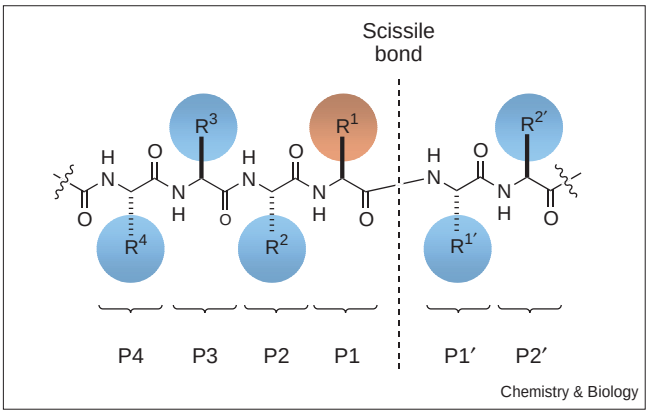

The catalytic sites of the proteasome accommodate multiple amino acid sidechains of the peptide substrate on both sides of the scissile bond.

the potency and subunit selectivity [16,24,25]. For example, introducing large hydrophobic sidechains in P4 of peptide vinyl sulfone inhibitors influences both potency and subunit selectivity [25], suggesting that sequence variation can be used to enhance subunit selectivity. Moreover, dihydroeponemycin (compare with eponemycin, Figure 1) shows no selectivity for the chymotrypsin-like activity over the PGPH activity, despite a leucine sidechain in P1 [23]. With the aim of designing potent inhibitors that have strong *in vivo* activity, it is likely that amino acids with hydrophobic sidechains in all positions as well as a *N*-acylated amino terminus would increase cell permeability and resistance to amino peptidases. We therefore focused on introducing different hydrophobic amino acids at P2–P4 of *N*-acetylated peptide α′,β′-epoxyketones with a leucine sidechain at P1 in order to provide important information on the structural features of proteasome inhibitors governing subunit selectivity and *in vivo* activity.

The peptide α′,β′-epoxyketones (compounds **1**–**18** in Tables 1–4) were assembled from left-hand peptide fragments (Figure 3a), prepared by standard solid-phase synthesis [37,38], and the previously described α′,β′-epoxyketone derived from leucine (Figure 3b) [21]. Variation in the size of sidechains in P2–P4 was accomplished by the use of alanine, leucine, phenylalanine, homophenylalanine, 3-(1-naphthyl)-alanine and *p*-benzoylphenylalanine as building blocks in the solid-phase peptide syntheses. Initially, the couplings between the left- and right-handed fragments (Figure 3) were carried out with *O*-(7-azabenzotriazol-1-yl)-1,1,3,3-tetramethyluronium hexafluorophosphate (HATU) [39] and diisopropylethylamine (DIEA) in dimethylformamide (DMF). When the products were analyzed using ^{1}H-nuclear magnetic resonance (NMR), however, some signals, most notably the signals from the hydrogens on C-1 of the epoxide, appeared in duplicate. The additional set of signals most likely originate from a minor stereoisomer (5–30%) formed by epimerization of the α carbon during the segment coupling (Figure 3). The minor epimers were difficult to remove using standard chromatography and poor overall yields were generally obtained. This undesired side reaction could be reduced but not eliminated by employing mixtures of DMF and dichloromethane as solvent and by using 2,4,6-trimethylpyridine (collidine) as base [40]. Purification using preparative normal phase high-performance liquid chromatography (HPLC) furnished the target peptide α′,β′-epoxyketones in good purity (typically >95%) and modest to good yields (20–70%).

Effect of the inhibitor length on inhibition of three catalytic activities of the 20S proteasome

As a first step, we investigated the potency of inhibitors of varying length. Mono-, di-, tri- and tetraleucine epoxides (compounds **1**–**4**, Table 1) were ranked by determining the k_{obs}/[I] value (Table 1) for inhibition of the chymotrypsin-like, trypsin-like and PGPH activities of purified bovine erythrocyte 20S proteasome. Tetrapeptide **1** showed strong inhibition of the chymotrypsin-like activity and had essentially no effect on the trypsin-like and PGPH activities. Truncation by one residue to give the tripeptide **2** resulted in a significantly reduced inhibition of the chymotrypsin-like activity with a small increase in the inhibition of the PGPH activity. Dipeptide **3** and the amino acid derivative **4** were found to be inactive against all three catalytic activities. Epoxomicin (Figure 1) is a very potent inhibitor of the chymotrypsin-like activity,

Figure 3

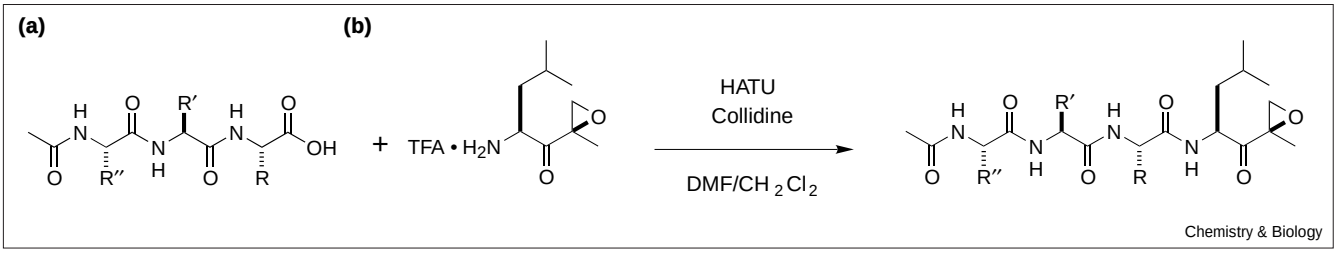

Synthesis of peptide α′,β′-epoxyketones by coupling of (a) peptide left-hand fragments to (b) the α′,β′-epoxyleucine right-hand fragment.

Table 1

Kinetic constants for inhibition of three catalytic activities of the proteasome by peptide α′,β′-epoxyketones of different length.

		$k_{obs}/[I]$ ($M^{-1}s^{-1}$)*		
		Chymotrypsin-like activity Suc-LLVY-AMC	Trypsin-like activity Boc-LRR-AMC	PGPH activity Z-LLE-AMC
1	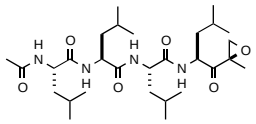	14,000 (50–150 nM)	–†	9.2 (100–160 μM)
2	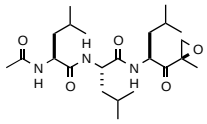	780 (1–2.5 μM)	5.1 (100–150 μM)	120 (8–12 μM)
3	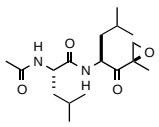	3.1 (100–160 μM)	–†	–†
4	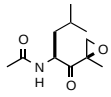	–†	–†	–†

*See the Materials and methods section for details. †Inhibition at 150 μM was either absent or insufficient to allow curve-fit to the collected data.

whereas dihydroeponemycin (compare with eponemycin, Figure 1), which lacks a P4 residue, shows modest inhibition of the same activity [22,23]. Taken together, these findings and the data in Table 1 suggest that the presence of a residue in P4 is important for strong inhibition of the chymotrypsin-like activity by peptide α′,β′-epoxyketones with a leucine sidechain in P1. This is in agreement with a recent study in which tripeptide vinyl sulfones were found to be less potent than tetrapeptide vinyl sulfones for inhibition of all three catalytic activities [25].

The tetraleucine epoxide **1** was chosen as a reference compound for the continuation of this study, in which the leucine residues in P2–P4 were substituted by different amino acids with aliphatic or aromatic sidechains of varying size.

Effect of amino acid substitutions in P2, P3 and P4 on inhibition of the three catalytic activities of the 20S proteasome

The leucine residues in P2 and P3 of the tetraleucine inhibitor **1** were substituted with alanine, phenylalanine or 3-(1-naphtyl)-alanine to give compounds **5**–**10**, respectively (Table 2). Compounds with aromatic sidechains in P2 and P3 increased the reactivity against the chymotrypsin-like activity with phenylalanine being optimal for P2 (compound **6**) and 3-(1-naphthyl)-alanine for P3 (compound **10**). Introduction of a phenylalanine residue in P2 furnished a highly potent inhibitor **6** with a $k_{obs}/[I]$ value exceeding the value previously reported for epoxomicin (Table 4) [22]. A recent study indicated a similar trend for dipeptide and tripeptide aldehydes and boronic acids where aromatic sidechains in P2 and P3 resulted in powerful inhibitors of the chymotrypsin-like activity [16].

The small and neutral alanine sidechain in P2 and P3 (compounds **5** and **8**) appears to be beneficial for inhibition of the trypsin-like and PGPH activity. The $k_{obs}/[I]$ values are relatively low, which make general predictions regarding sidechain size in P2 and P3 and inhibition of the trypsin-like and PGPH activities uncertain. Compound **8**, which has an alanine residue in P3, is, however, more potent for inhibition of the PGPH activity than, for example, the previously reported compounds epoxomicin [22], eponemycin [23], 4-hydroxy-2-iodo-5-nitrophenyl-acetyl-leucinyl-leucinyl-leucine vinyl sulfone (NLVS) [25], and *clasto*-lactacystin β-lactone [15] (Table 4). The boronic acid PS-341 [16] (Table 4) is, however, by far the most potent inhibitor of the PGPH activity reported so far.

The next step was to investigate the effects of large aromatic sidechains on the three catalytic activities when placed in P4. In a recent study of peptide vinyl sulfones, the presence and size of this sidechain had a substantial impact on the reactivity against all three catalytic activities [25]. To address the structural requirements of the P4 pocket in somewhat greater detail, we included the building blocks homophenylalanine and *p*-benzoylphenylalanine, in addition to alanine, leucine, phenylalanine and 3-(1-naphthyl)-alanine, which were used for

Table 2

Kinetic constants for inhibition of three catalytic activities of the proteasome by peptide α′,β′-epoxyketones with various amino acids in P2 and P3.

	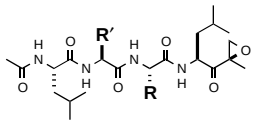	$k_{obs}/[I]$ ($M^{-1}s^{-1}$)*		
		Chymotrypsin-like activity Suc-LLVY-AMC	Trypsin-like activity Boc-LRR-AMC	PGPH activity Z-LLE-AMC
1	R′ =  R = 	14,000 (50–150 nM)	–†	9.2 (100–160 μM)
5	 	16,000 (80–120 nM)	4.1 (100–150 μM)	20 (60–80 μM)
6	 	54,000 (40–60 nM)	–†	–†
7	 	29,000 (60–120 nM)	–†	–†
8	 	1300 (500–1000 nM)	2.0 (120–150 μM)	130 (10–16 μM)
9	 	8500 (200–400 nM)	–†	–†
10	 	31,000 (40–100 nM)	–†	–†

*See the Materials and methods section for details. †Inhibition at 150 μM was either absent or insufficient to allow curve-fit to the collected data

the compounds in Table 2. The resulting set of P4 analogs (compounds **11**–**15**, Table 3) all showed strong inhibition of the chymotrypsin-like activity with a clear sidechain size optimum. Compound **11**, containing an alanine in P4, had a lower $k_{obs}/[I]$ value than the tetraleucine inhibitor **1** for the inhibition of the chymotrypsin-like activity. Inhibitors **12**–**15** with aromatic sidechains in P4 all exhibited improved inhibition of the chymotrypsin-like activity with $k_{obs}/[I]$ in the same order of magnitude as epoxomicin (Table 4) [22]. Homophenylalanine in P4 (**13**) proved to be the most active inhibitor with similar potency to compound **6** (Table 2), which contains a phenylalanine residue in P2. These data, however, do not reveal any clear trends for the trypsin-like and PGPH activities for which the inhibitors are either poor or inactive. Introduction of large aromatic sidechains, as in compounds **14** and **15** with 3-(1-naphtyl)-alanine and *p*-benzoylphenylalanine in P4, resulted in inactive derivatives, whereas the alanine, phenylalanine and homophenylalanine inhibitors **11**–**13** caused a modest reduction of the trypsin-like and PGPH activities. Inhibition of the PGPH activity appeared to benefit from small sidechain residues, that is the alanine derivative **11**, which is somewhat more active than the P3 alanine inhibitor **8** (Table 2). The ranking of compounds **1** and **11**–**15** (Table 3) is based on data collected with 20S bovine erythrocyte proteasome. Investigating these inhibitors with 20S proteasome from bovine brain resulted in the same ranking and similar absolute $k_{obs}/[I]$ values (data not shown).

The data in Tables 2 and 3 clearly indicate that the potency of tetrapeptide α′,β′-epoxyketones for inhibition of the chymotrypsin-like activity is enhanced by introduction of aromatic sidechains in P2–P4. Several of the compounds, most notably **6** and **13** (Tables 2 and 3) are excellent inhibitors of the chymotrypsin-like activity. Our results, however, suggest that for this class of inhibitors,

Table 3

Kinetic constants for inhibition of three catalytic activities of the proteasome by peptide α′,β′-epoxyketones with various amino acids in P4.

	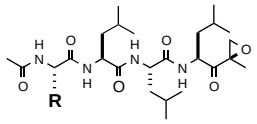	$k_{obs}/[I]$ ($M^{-1}s^{-1}$)*		
		Chymotrypsin-like activity Suc-LLVY-AMC	Trypsin-like activity Boc-LRR-AMC	PGPH activity Z-LLE-AMC
11	R= 	5300 (400–800 nM)	3.8 (100–150 μM)	220 (8–12 μM)
1		14,000 (50–100 nM)	–†	9.2 (100–160 μM)
12		37,000 (40–80 nM)	5.5 (100–150 μM)	78 (20–40 μM)
13		63,000 (40–80 nM)	5.4 (120–150 μM)	50 (30–50 μM)
14		29,000 (60–120 nM)	–†	–†
15	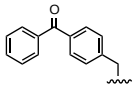	23,000 (90–150 nM)	–†	–†

*See the Materials and methods section for details. †Inhibition at 150 μM was either absent or insufficient to allow curve-fit to the collected data.

that is peptide α′,β′-epoxyketones with leucine in P1, improvement of inhibition of the trypsin-like and PGPH activities and simultaneous reduction of inhibition of the chymotrypsin-like activity might be difficult to achieve.

Synthesis and evaluation of an optimized inhibitor

The results in Table 1–3 clearly show that variation of residues in P2–P4 of peptide α′,β′-epoxyketones with leucine in P1 have a major impact on inhibition of the chymotrypsin-like activity. Our efforts next focused on the synthesis of a second generation inhibitor with increased inhibition of the chymotrypsin-like activity. Phenylalanine in P2 (**6**, Table 2) and homophenylalanine in P4 (**13**, Table 3) showed major enhancements in potency, so inhibitor **16** (Table 4) with a combination of these residues was prepared. As expected, compound **16** was found to exhibit remarkable selectivity and potency for inhibition of the chymotrypsin-like activity. Moreover, compound **16** is more powerful and selective for the chymotrypsin-like activity than the previously characterized inhibitors epoxomicin [22], dihydroeponemycin [23], the boronic acid PS-341 [16], *clasto*-lactacystin β-lactone [15] and NLVS [25,26] (Table 4).

Because epoxomicin selectively targets the proteasome without concomitant inhibition of other proteases such as trypsin, chymotrypsin, papain, calpain and cathepsin B at concentrations up to 50 μM [22], it can be assumed that the peptide α′,β′-epoxyketone **16** exhibits a similar selectivity pattern. Roush *et al.* [41] recently described the synthesis and evaluation of two *N*-protected dipeptide α′,β′-epoxyketones with excellent activity against the cysteine protease cruzain. Interestingly, inhibitors with 2-(*S*)-stereochemistry of the epoxide were found to be substantially more active than the corresponding 2-(*R*)-derivatives. However, potent proteasome inhibitors in this and previous studies [20–23] exclusively have the 2-(*R*)-configuration. In two investigations, the corresponding 2-(*S*)-derivatives were tested and found to be considerably less potent for inhibition of the proteasome [20,21]. Apparently, the stereochemistry of the epoxide plays an important role in selectivity for the proteasome over other proteases.

To date, the most detailed investigation of sidechain effects on proteasome specificity was carried out with P4 variants of peptide vinyl sulfones [25]. The inhibitors

Table 4

Kinetic constants for inhibition of three catalytic activities of the proteasome by 16, 18, epoxomicin, PS-341, NLVS, and *clasto*-lactacystin β-lactone.

		$k_{obs}/[I]$ ($M^{-1}s^{-1}$)*		
		Chymotrypsin-like activity Suc-LLVY-AMC	Trypsin-like activity Boc-LRR-AMC	PGPH activity Z-LLE-AMC
16	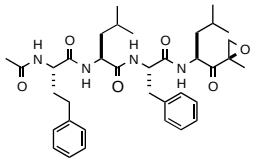	166,000 (5–12 nM)	7.1 (80–130 μM)	21 (80–150 μM)
18	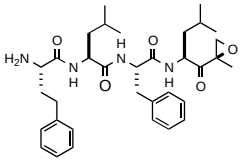	5200 (0.11 μM)	580 (0.5–5 μM)	11 (10–150 μM)
	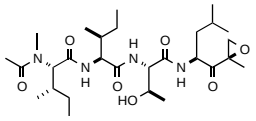 Epoxomicin	37,000 (30–80 nM)	79 (8–12 μM)	37 (50–100 μM)
	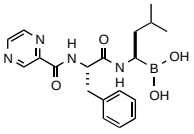 PS-341	53,000 (30–10 nM)	150 (5–35 μM)	3200 (0.3–1 μM)
	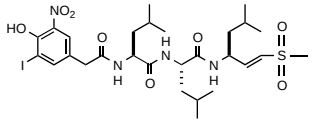 NLVS	5000 (200–500 nM)	3.4 (50–120 μM)	4.0 (50–100 μM)
	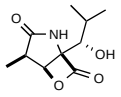 *clasto*-Lactacystin β-lactone	7400 (150–500 nM)	68 (8–12 μM)	47 (30–80 μM)

*See the Materials and methods section for details.

studied had a free amino terminus in order to mimic peptide substrates that had already undergone one or more cycles of hydrolytic cleavage. To address whether a free or acetylated amino terminus of peptide α′,β′-epoxyketones can effect subunit preference and potency, we prepared compound **18** from the Fmoc protected precursor **17** (Figure 4). Evaluation of inhibitor **18** (Table 4), which is a deacetylated derivative of the powerful inhibitor **16**, revealed a dramatic reduction in inhibition of the chymotrypsin-like activity indicating a subunit preference for longer substrates or inhibitors. Compound **18** also exhibited a major increase in potency for inhibition of the trypsin-like activity with a higher $k_{obs}/[I]$ value than the *N*-capped inhibitors (Tables 1–3), epoxomicin [22], eponemycin [23], NLVS [25] and *clasto*-lactacystin β-lactone [15] (Table 4). Both **16** and **18** are weak inhibitors of the PGPH activity (Table 4). The differences observed between inhibitors **16** and **18** corroborate the results obtained in the vinyl sulfone study in which uncapped inhibitors were less potent against the chymotrypsin-like activity and more active against the trypsin-like activity when compared with NLVS [25]. It is interesting to speculate that the proteolytic machinery of the proteasome may work in a sequential manner, namely the chymotrypsin-like activity

Figure 4

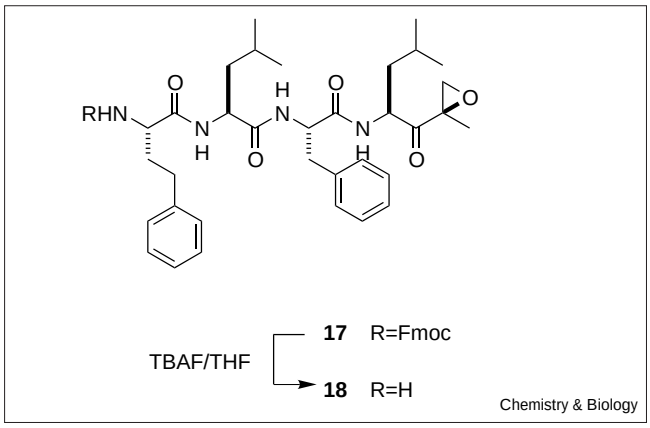

Synthesis of a peptide α′,β′-epoxyketone with an unprotected amino terminus.

Figure 5

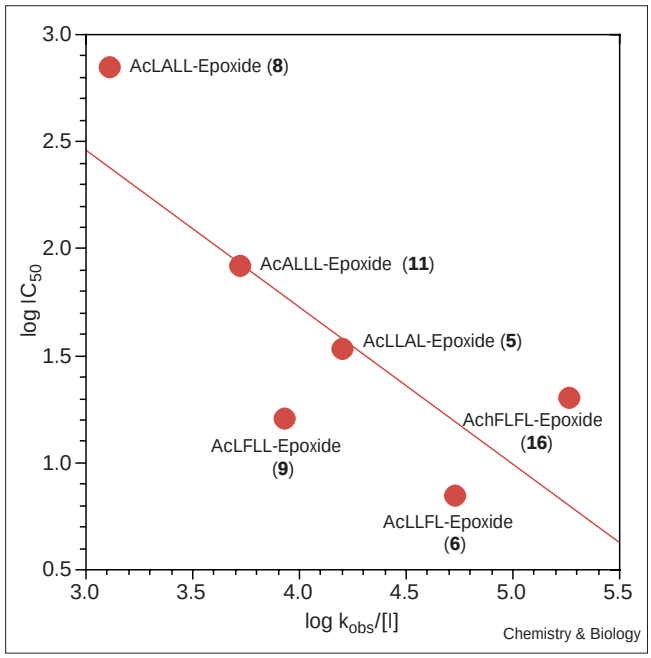

Correlation of log k_{obs}/[I] values for inhibition of the chymotrypsin-like activity of the proteasome with log IC_{50} values for inhibition of bovine aortic endothelial (BAE) cell proliferation by a subset of peptide α′,β′-epoxyketones.

cleaves initial longer substrates followed by continued hydrolysis of the resulting shorter peptides by the trypsin-like and PGPH activities. This argument is, in part, supported by the fact that shorter inhibitors such as the trileucine compound **2** (Table 1), dihydroeponemycin [23], and the dipeptidyl boronic acid PS-341 [16] (Table 4) can inhibit the PGPH activity and, in some cases, do so better than longer inhibitors.

The data for our novel peptide α′,β′-epoxyketones presented in Tables 1–4 reflect the importance of inhibitor length and a clear cooperative effect of the sidechains in different positions of peptide-based inhibitors with an α′,β′-epoxyketone pharmacophore. Modifications, such as the introduction of other amino acid residues in P1–P4, addition of P1′ residues and a free amino terminus will further add to our understanding of substrate recognition by the 20S proteasome. Although introduction of polar or charged residues and a free amino terminus might enhance selectivity and potency for inhibition of the trypsin-like and PGPH activities, these chemical modifications can be expected to result in lower membrane permeability, which is important for *in vivo* activity.

Table 5

Values of k_{obs}/[I] for inhibition of the chymotrypsin-like activity and IC_{50} values for inhibition of BAE cell proliferation for a subset of peptide α′,β′-epoxyketones.

Inhibitor	K_{obs}/[I] (M^{-1} s^{-1})*	IC_{50} (nM)†
5 Ac-LLAL-epoxide	16,000	34
6 Ac-LLFL-epoxide	54,000	7
8 Ac-LALL-epoxide	1300	700
9 Ac-LFLL-epoxide	8500	16
11 Ac-ALLL-epoxide	5300	83
16 Ac-hFLFL-epoxide	166,000	20

*See the Materials and methods section for details. †Approximately 1000 BAE cells were plated into each well of a 96-well culture plate. After an overnight incubation, different concentrations of proteasome inhibitors were added and incubation was continued for another 5 days. Subsequently, [methyl-^{3}H]-thymidine was added to the plate and incubated for an additional 4 h. Cells were harvested and incorporated radioactivity was quantified using liquid scintillation.

Correlation of inhibition of the chymotrypsin-like activity and growth inhibition of bovine aortic endothelial cells

In this study, we demonstrate that peptide α′,β′-epoxyketones with enhanced reactivity against the chymotrypsin-like activity of the 20S proteasome can be prepared by amino acid sidechain substitutions in P2–P4. In order to address if these *in vitro* data can be translated to biological function *in vivo*, inhibition of cell proliferation of bovine aortic endothelial (BAE) cells was investigated with a subset of our novel peptide α′,β′-epoxyketones. Proliferation of BAE cells was assayed in triplicate in the presence of different concentrations of peptide α′,β′-epoxyketones. After 5 days, all inhibitors consistently inhibited cell growth in a dose-dependent manner. As illustrated in Table 5 and Figure 5, a higher k_{obs}/[I] value for inhibition of the chymotrypsin-like activity of the proteasome generally corresponds to a lower IC_{50} value for inhibition of cell proliferation. The absence of a strict correlation between k_{obs}/[I] and IC_{50} values most likely reflects the greater

Figure 6

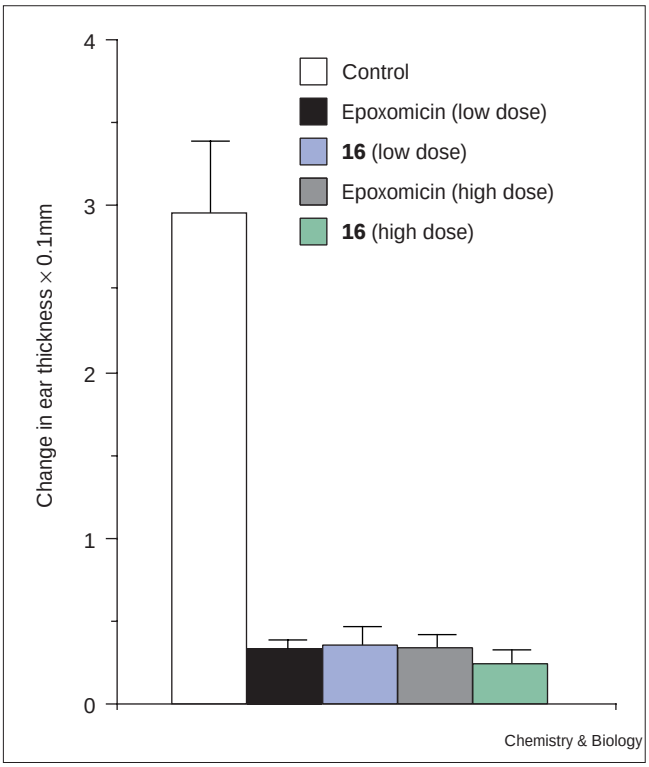

Irritant sensitivity response to 2,4-dinitrofluorobenzene (DNFB). BALB/c mice were injected with epoxomicin (0.32 mg or 2.0 mg/kg body weight), inhibitor **16** (0.37 or 2.3 mg/kg body weight) or with vehicle (10% DMSO in buffered saline) prior to ear challenge with 0.3% DNFB. The low dose corresponds to 0.58 μmol/kg and the high dose to 3.6 μmol/kg for both epoxomicin and **16**. Ear swelling measurements of both ears were made 0 h and 24 h post-ear challenge with an engineer's micrometer. Results are expressed as 24 h ear thickness measurement minus 0 h ear thickness measurement.

complexity of a cell-based assay than that of an *in vitro* assay with purified proteasome. It is also possible that inhibitors with lower $k_{obs}/[I]$ values cause substantial inhibition of cellular proteasomes during experiments conducted over longer times because the $k_{obs}/[I]$ values indicate the rate of enzyme inactivation. Potent inhibitors with $k_{obs}/[I]$ values greater than 8,000 $M^{-1}s^{-1}$ gave IC_{50} values in the range of 7–34 nM. The trend observed in Figure 5 suggests that the proteasome is the true biological target for this powerful class of inhibitors.

Epoxomicin and Ac-hFLFL-epoxide (16) exhibit potent anti-inflammatory activity *in vivo*

Haptens such as 2,4,6-trinitrochlorobenzene (picryl chloride) and 2,4-dinitrofluorobenzene (DNFB) elicit nonspecific irritant sensitivity responses within 24 hours after contact in the mouse ear edema assay [42]. On the basis of our previous observation that epoxomicin potently inhibited NF-κB activation in tumor necrosis factor α (TNF-α)-stimulated cells and demonstration of *in vivo* anti-inflammatory activity in the contact sensitivity assay [22], we investigated the pharmacological activities of the optimized inhibitor **16** in the DNFB ear edema model of irritant sensitivity. Mice were injected with either a low dose (0.32 mg/kg) or a high dose (2.0 mg/kg) of epoxomicin, the inhibitor **16** (0.37 and 2.3 mg/kg), or vehicle (10% DMSO) one hour prior to applying DNFB to the ear. The low dose corresponds to 0.58 μmol/kg and the high dose to 3.6 μmol/kg for both epoxomicin and **16**. Ear thickness was measured at 0 and 24 hours after DNFB application. As shown in Figure 6, a single dose of epoxomicin at 2.0 mg/kg inhibited ear inflammation by ninefold over that of vehicle-treated controls. Interestingly, a sixfold lower amount of epoxomicin decreased inflammation by this same margin. A low dose of optimized inhibitor **16** also exerted potent anti-inflammatory activity, reducing ear swelling by the same amount as epoxomicin. At the higher dose, the inhibitor **16** decreased ear swelling by 12-fold, demonstrating a small but higher level of potency compared to epoxomicin. The natural product epoxomicin and **16**, which is optimized for inhibition of the chymotrypsin-like activity of the proteasome, therefore, both exhibit potent anti-inflammatory activities *in vivo*. Furthermore, these results indicate that for this class of inhibitors strong *in vitro* proteasome inhibition correlates with strong *in vivo* activities, as illustrated by the anti-proliferative and anti-inflammatory activities. The inhibitor **16** and the inhibitors used in the cell proliferation assays are selective for inhibition of the chymotrypsin-like activity suggesting that inhibition of this activity is sufficient to cause a biological effect such as growth arrest and anti-inflammatory activity *in vivo*.

Significance

The proteasome is a multicatalytic proteolytic complex responsible for ubiquitin-dependent protein degradation. Given the importance of the proteasome in normal physiological and disease states, compounds that inhibit the proteasome *in vitro* and *in vivo* are needed as molecular probes for understanding proteasome biology and as potential therapeutic compounds. In addition to the biological potency, inhibitors should be selective for the proteasome and preferably for one of the three major proteasomal catalytic activities. In this study, we have synthesized and evaluated a panel of peptide α′,β′-epoxyketones based on the natural product epoxomicin that exhibit antitumor and anti-inflammatory activity through inhibition of the proteasome. All inhibitors contained a leucine residue in the P1 position and were found to be good or excellent inhibitors of the chymotrypsin-like activity and poor inhibitors of the trypsin-like and post-glutamyl peptide hydrolyzing (PGPH) activities. Introduction of different aliphatic and aromatic residues in P2–P4 had a dramatic impact on the inhibition of the chymotrypsin-like activity. Inhibition of the chymotrypsin-like activity could be correlated

with inhibition of cell proliferation indicating that the biological effect is mediated by proteasome inhibition. Optimization furnished an inhibitor, Ac-hFLFL-epoxide, that proved to be more potent and selective for inhibition of the chymotrypsin-like activity than several previously described inhibitors. Furthermore, the optimized inhibitor exhibits strong anti-inflammatory activity in a contact irritant sensitivity assay in mice. Taken together our results show that amino acid substitutions in different positions of proteasome inhibitors can be used to enhance both *in vitro* and *in vivo* activity of peptide α′,β′-epoxyketones. This family of inhibitors constitutes a valuable class of molecular probes for understanding proteasome biology and as therapeutic agents that target proteasome functions in different stages of disease.

Materials and methods

General

Peptides were synthesized by standard solid-phase peptide synthesis [37,38] starting from commercially available N^{α}-fluoren-9-ylmethoxycarbonyl (Fmoc) amino acid Wang resins except for the peptide with 3-(1-naphtyl)-alanine as carboxy-terminal amino acid, which was synthesized from a 2-chlorotrityl chloride resin. N^{α}-Fmoc and N^{α}-acetyl amino acids were coupled in DMF with O-benzotriazol-1-yl-*N*,*N*,*N*′,*N*′-tetramethyluronium hexafluorophosphate (HBTU) and DIEA, or HATU and DIEA. Fmoc groups were removed with 20% piperidine in DMF and final cleavage from the solid support was effected by trifluoroacetic acid:water (95:5). DMF was distilled under reduced pressure and stored over 4 Å molecular sieves. Dichloromethane was passed through a short column of neutral Al_2O_3 (activity 1) and stored over 4 Å molecular sieves. Flash column chromatography was performed with EM Science silica gel 60 (230–400 mesh) and thin layer chromatography (TLC) was carried out with Merck silica gel 60 (0.25 mm) F254 precoated glass plates with appropriate hexanes-ethylacetate or dichloromethane-methanol systems. TLC plates were stained by heating with phosphomolybdic acid in ethanol. Preparative HPLC was performed with a Rainin Dynamax system with a Microsorb silica column (100 Å, 5 μm, 21.4 × 250 mm) and UV detection (214 nm) with appropriate gradients of isopropanol in hexanes (15–20 ml/min). ^{1}H-NMR spectra were recorded with a Bruker AM-500 spectrometer at 500 MHz in $CDCl_3$ (δ_H 7.27), acetone-d_6 (δ_H 2.05) or DMSO-d_6 (δ_H 2.49). Electrospray (ES) mass spectra were recorded at the Yale Cancer Center Mass Spectrometry Resource and the W.M. Keck Foundation Biotechnology Resource Laboratory, New Haven, CT, USA. In addition to signals corresponding to $(M + H)^+$, signals originating from $(M + Na)^+$ and $(M + K)^+$ were frequently observed. Epoxomicin (Figure 1) and the right-hand fragment (2*R*,4*S*)-4-amino-2,6-dimethyl-hept-1,2-epoxy-3-one (Figure 3b) were prepared essentially as described previously [21]. Fmoc amino acids and resins were purchased from Advanced ChemTech and HATU from PerSeptive Biosystems. NLVS and *clasto*-lactacystin β-lactone were obtained from CalBiochem and 2,4-dinitrofluorobenzene (DNFB) was purchased from Sigma Chemical Co. Proteasome substrates were obtained from Bachem and Peptides International. [Methyl-^{3}H]-thymidine was purchased from NEN Science Products, Inc.

General protocol for synthesis of peptide α′,β′-epoxyketones

The left-hand peptide fragment (104 μmol, Figure 3a) was dissolved in DMF (0.2–0.3 ml) and the trifluoroacetate ammonium salt of (2*R*,4*S*)-4-amino-2,6-dimethyl-hept-1,2-epoxy-3-one (15 mg, 52 μmol, Figure 3b) in dichloromethane (1.5 ml) was added. Collidine (2,4,6-trimethylpyridine, 26 μl, 208 μmol) and HATU (40 mg, 104 μmol) were added and the resulting mixture was stirred at room temperature. After 3–4 h the solution was concentrated under reduced pressure and the residue was flash chromatographed (dichloromethane–methanol) to give partially purified product. The peptide α′,β′-epoxyketone was isolated (typically > 95% purity in 20–70% yield) by preparative normal phase HPLC (gradient of isopropanol in hexanes).

*Selected ^{1}H-NMR and ESMS data for compounds **1–17***

1: ^{1}H-NMR δ (DMSO-d_6) 8.04 (d, *J* = 7.0 Hz, 1 H), 8.00 (d, *J* = 8.5 Hz, 2 H), 7.70 (d, *J* = 9.0 Hz, 1 H), 4.34–4.20 (m, 4 H), 3.17 (d, *J* = 5.5 Hz, 1 H), 2.99 (d, *J* = 5.0 Hz, 1 H), and 1.81 (s, 3 H); ESMS $(M + H)^+$ calc'd 553.40, found 553.35.

2: ^{1}H-NMR δ (DMSO-d_6) 7.99 (d, *J* = 7.5 Hz, 1 H), 7.95 (d, *J* = 8.0 Hz, 1 H), 7.84 (d, *J* = 9.0 Hz, 1 H),4.39–4.23 (m, 3 H), 3.16 (d, *J* = 5.0 Hz, 1 H), 2.98 (d, *J* = 5.0 Hz, 1 H), and 1.81 (s, 3 H); ESMS $(M + H)^+$ calc'd 440.31, found 440.39.

3: ^{1}H-NMR δ ($CDCl_3$) 6.35 (d, *J* = 7.5 Hz, 1 H), 5.89 (d, *J* = 8.0 Hz, 1 H), 4.56 (ddd, *J* = 3.1, 7.4, and 10.4 Hz, 1 H), 4.46 (ddd, *J* = 5.5 and 8.5 Hz, 1 H), 3.30 (d, J = 5.0 Hz, 1 H), 2.90 (d, J = 5.5 Hz, 1 H), 1.99 (s, 3 H), and 1.52 (s, 3 H); ESMS $(M + H)^+$ calc'd 327.23, found 327.27.

4: ^{1}H-NMR δ ($CDCl_3$) 5.80–5.75 (m, 1 H), 4.68–4.64 (m, 1 H), 3.35 (d, *J* = 4.5 Hz, 1 H), 2.90 (d, *J* = 5.0 Hz, 1 H), 1.99 (s, 3 H), 1.52 (s, 3 H), 0.98 (d, *J* = 7.0 Hz, 3 H), and 0.95 (d, *J* = 6.5 Hz, 3 H); ESMS $(M + H)^+$ calc'd 214.15, found 214.17.

5: ^{1}H-NMR δ (DMSO-d_6) 8.07 (d, *J* = 7.5 Hz, 1 H), 7.96 (d, *J* = 8.0 Hz, 1 H), 7.91 (d, *J* = 8.5 Hz, 1 H), 7.73 (d, *J* = 7.0 Hz, 1 H), 4.34–4.29 (m, 1 H), 4.27–4.20 (m, 3 H), 3.17 (d, *J* = 5.5 Hz, 1 H), 3.00 (d, *J* = 5.0 Hz, 1 H), 1.82 (s, 3 H), 1.39 (s, 3 H), and 1.14 (d, *J* = 7.0 Hz, 3 H); ESMS $(M + H)^+$ calc'd 511.35, found 511.44.

6: ^{1}H-NMR δ (DMSO-d_6) 8.19 (d, *J* = 7.0 Hz, 1 H), 7.95 (d, *J* = 8.0 Hz, 1 H), 7.89 (d, *J* = 8.5 Hz, 1 H), 7.72 (d, *J* = 8.0 Hz, 1 H), 7.23–7.14 (m, 5 H), 4.53–4.48 (m, 1 H), 4.38–4.33 (m, 1 H), 4.24–4.15 (m, 2 H), 3.14 (d, *J* = 6.0 Hz, 1 H), 2.98 (d, *J* = 5.5 Hz, 1 H), 2.96 (dd, *J* = 5.0 and 16.0 Hz, 1 H), 2.74 (dd, *J* = 8.8 and 13.8 Hz, 1 H), 1.81 (s, 3 H), and 1.39 (s, 3 H); ESMS $(M + H)^+$ calc'd 587.38, found 587.50.

7: ^{1}H-NMR δ (DMSO-d_6) 8.15 (bt, *J* = 6.8 Hz, 2 H), 7.98 (d, *J* = 8.0 Hz, 1 H), 7.93 (d, *J* = 7.5 Hz, 1 H), 7.89 (bt, *J* = 7.0 Hz, 2 H), 7.76 (d, *J* = 8.0 Hz, 1 H), 7.57–7.49 (m, 2 H), 7.35 (t, *J* = 7.8 Hz, 1 H), 7.27 (d, *J* = 7.0 Hz, 1 H), 4.67–4.63 (m, 1 H), 4.41–4.36 (m, 1 H), 4.24–4.13 (m, 2 H), 3.43 (dd, *J* = 5.5 and 14.5 Hz, 1 H), 3.20–3.16 (m, 2 H), 3.00 (d, *J* = 5.0 Hz, 1 H), and 1.82 (s, 3 H); ESMS $(M + H)^+$ calc'd 637.40, found 637.55.

8: ^{1}H-NMR δ (DMSO-d_6) 8.07 (d, *J* = 7.0 Hz, 1 H), 8.06 (d, *J* = 7.0 Hz, 1 H), 7.98 (d, *J* = 8.0 Hz, 1 H), 7.62 (d, *J* = 8.5 Hz, 1 H), 4.33–4.19 (m, 4 H), 3.17 (d, *J* = 5.0 Hz, 1 H), 2.99 (d, *J* = 5.5 Hz, 1 H), 1.82 (s, 3 H), 1.38 (s, 3 H), and 1.16 (d, *J* = 7.5 Hz, 3 H); ESMS $(M + H)^+$ calc'd 511.35, found 511.46.

9: ^{1}H-NMR δ (DMSO-d_6) 8.13 (d, *J* = 6.5 Hz, 1 H), 7.97 (d, *J* = 8.0 Hz, 1 H), 7.95 (d, *J* = 10.0 Hz, 1 H), 7.80 (d, *J* = 8.5 Hz, 1 H), 7.22–7.14 (m, 5 H), 4.48–4.43 (m, 1 H), 4.34–4.28 (m, 2 H), 4.18 (bdd, *J* = 7.5 and 15.5 Hz, 1 H), 3.19 (d, *J* = 5.0 Hz, 1 H), 3.04–2.98 (m, 1 H), 2.79 (dd, *J* = 9.2 and 13.8 Hz, 1 H), 1.78 (s, 3 H), and 1.39 (s, 3 H); ESMS $(M + H)^+$ calc'd 587.38, found 587.51.

10: ^{1}H-NMR δ (DMSO-d_6) 8.14 (d, *J* = 8.5 Hz, 1 H), 8.11 (d, *J* = 8.5 Hz, 1 H), 8.07 (d, *J* = 7.0 Hz, 1 H), 7.90 (bt, *J* = 8.2 Hz, 2 H), 7.77 (bt, *J* = 8.0 Hz, 2 H), 7.56–7.49 (m, 2 H), 7.36–7.31 (m, 2 H), 4.60 (ddd, *J* = 4.7 and 9.0 Hz, 1 H), 4.38–4.30 (m, 2 H), 4.15 (bdd, *J* = 8.0 and 15.0 Hz, 1 H), 3.54 (dd, *J* = 5.0 and 14.5 Hz, 1 H), 3.21 (dd, *J* = 10.0 and 15 Hz, 1 H), 3.19 (d, *J* = 5.5 Hz, 1 H), 2.99 (d, *J* = 5.5 Hz, 1 H), 1.78 (s, 3 H), and 1.39 (s, 3 H); ESMS $(M + H)^+$ calc'd 637.40, found 637.52.

11: ^{1}H-NMR δ (DMSO-d_6) 8.03–8.02 (m, 2 H), 7.90 (d, *J* = 8.0 Hz, 1 H), 7.71 (d, *J* = 8.5 Hz, 1 H), 4.34–4.19 (m, 4 H), 3.16 (d, *J* = 5.0 Hz, 1 H), 2.99 (d, *J* = 5.5 Hz, 1 H), 1.81 (s, 3 H), 1.38 (s, 3 H), and 1.14 (d, *J* = 7.5 Hz, 3 H); ESMS (M + H)$^+$ calc'd 511.35, found 511.29.

12: ^{1}H-NMR δ (DMSO-d_6) 8.08–8.03 (m, 3 H), 7.81 (d, *J* = 8.5 Hz, 1 H), 7.24–7.23 (m, 4 H), 7.18–7.16 (m, 1 H), 4.48 (ddd, *J* = 4.0, 8.2, and 9.8 Hz, 1 H), 4.35–4.25 (m, 3 H), 3.14 (d, *J* = 5.0 Hz, 1 H), 2.96 (d, *J* = 5.5 Hz, 1 H), 2.95 (dd, *J* = 4.0 and 12.8 Hz, 1 H), 2.69 (dd, *J* = 9.8 and 13.8 Hz, 1 H), 1.73 (s, 3 H), and 1.38 (s, 3 H); ESMS (M + H)$^+$ calc'd 587.38, found 587.24.

13: ^{1}H-NMR δ (DMSO-d_6) 8.09 (d, *J* = 8.0 Hz, 1 H), 8.02 (d, *J* = 7.0 Hz, 1 H), 7.99 (d, *J* = 8.5 Hz, 1 H), 7.77 (d, *J* = 9.0 Hz, 1 H), 7.27–7.15 (m, 5 H), 4.32–4.22 (m, 4 H), 3.13 (d, *J* = 5.0 Hz, 1 H), 2.96 (d, *J* = 5.0 Hz, 1 H), 2.57–2.50 (m, 2 H), 1.85 (s, 3 H), and 1.38 (s, 3 H); ESMS (M + H)$^+$ calc'd 601.40, found 601.38.

14: ^{1}H-NMR δ (DMSO-d_6) 8.17 (d, *J* = 7.5 Hz, 2 H), 8.12 (d, *J* = 8.0 Hz, 1 H), 8.09 (d, *J* = 6.5 Hz, 1 H), 7.9 (bd, *J* = 7.5 Hz, 1 H), 7.81 (d, *J* = 8.0 Hz, 1 H), 7.77 (bt, *J* = 4.8 Hz, 1 H), 7.56–7.50 (m, 2 H), 7.40–7.38 (m, 2 H), 4.68–4.64 (m, 1 H), 4.36–4.30 (m, 3 H), 3.49 (dd, *J* = 4.0 and 15.0 Hz, 1 H), 3.13 (dd, J = 9.5 and 14.0 Hz, 1 H), 3.12 (d, *J* = 5.0 Hz, 1 H), 2.91 (d, *J* = 5.5 Hz, 1 H), 1.71 (s, 3 H), and 1.37 (s, 3 H); ESMS (M + H)$^+$ calc'd 637.40, found 637.35.

15: ^{1}H-NMR δ (acetone-d_6) 7.77–7.76 (m, 2 H), 7.71 (bd, J = 8.0 Hz, 2 H), 7.68–7.64 (m, 2 H), 7.57–7.52 (m, 3 H), 7.47–7.43 (m, 3 H), 7.34 (d, *J* = 7.0 Hz, 1 H), 4.70–4.66 (m, 1 H), 4.54–4.50 (m, 1 H), 4.45–4.37 (m, 2 H), 3.31 (d, *J* = 5.0 Hz, 1 H), 3.27 (dd, *J* = 5.0 and 14.0 Hz, 1 H), 3.11 (dd, *J* = 7.8 and 13.8 Hz, 1 H), 2.92 (d, *J* = 5.5 Hz, 1 H), 1.91 (s, 3 H), and 1.43 (s, 3 H); ESMS (M + H)$^+$ calc'd 691.41, found 691.38.

16: ^{1}H-NMR δ (DMSO-d_6) 8.21 (d, *J* = 7.5 Hz, 1 H), 8.10 (d, *J* = 8.0 Hz, 1 H), 7.96 (d, *J* = 8.0 Hz, 1 H), 7.84 (d, *J* = 8.0 Hz, 1 H), 7.23 (bt, *J* = 7.5 Hz, 2 H), 7.20–7.06 (m, 8 H), 4.51 (ddd, *J* = 4.8 and 8.8 Hz, 1 H), 4.36–4.31 (m, 1 H), 4.24–4.19 (m, 2 H), 3.09 (d, *J* = 5.5 Hz, 1 H), 2.95 (dd, *J* = 4.5 and 14.0 Hz, 1 H), 2.94 (d, *J* = 4.5 Hz, 1 H), 2.73 (dd, *J* = 9.2 and 14.2 Hz, 1 H), 2.58–2.46 (m, 2 H), 1.85 (s, 3 H), 1.38 (s, 3 H), 0.86 (d, *J* = 6.5 Hz, 3 H), 0.83 (d, *J* = 7.0 Hz, 3 H), and 0.78 (bt, *J* = 6.8 Hz, 6 H); ESMS (M + H)$^+$ calc'd 635.38, found 635.40.

17: ^{1}H-NMR δ (acetone-d_6) 7.87 (d, *J* = 7.5 Hz, 2 H), 7.70 (dd, *J* = 7.8 and 11.2 Hz, 2 H), 7.60 (bs, 1 H), 7.47 (d, *J* = 8.5 Hz, 1 H), 7.74–7.08 (m, 11 H), 7.00 (bs, 1 H), 4.64 (ddd, *J* = 4.7 and 8.6 Hz, 1 H), 4.56–4.46 (m, 2 H), 4.38–4.24 (m, 3 H), 4.16 (dd, *J* = 6.0 and 13.5 Hz, 1 H), 3.28 (d, *J* = 5.0 Hz, 1 H), 3.20 (dd, *J* = 4.8 and 14.2 Hz, 1 H), 2.91 (d, *J* = 5.5 Hz, 1 H), 2.90 (dd, *J* = 5.0 and 16.2 Hz, 1 H), 2.78–2.66 (m, 2 H), 1.44 (s, 3 H), 0.87 (bt, *J* = 6.0 Hz, 6 H), and 0.82 (bt, *J* = 6.2 Hz, 6 H); ESMS (M + H)$^+$ calc'd 815.44, found 815.47.

*Synthesis of compound **18***

Compound **17** (11 mg, 13.5 μmol) was dissolved in tetrahydrofuran (1 ml) and tetrabutylammonium fluoride (40 μl, 20 μmol, 0.5 M in tetrahydrofuran) was added. The resulting solution was stirred at room temperature for 70 min. Approximately half of the solvent was removed by evaporation under reduced pressure and the remaining solution was chromatographed (dichloromethane–methanol, 20:1) to give **18** (5.2 mg, 65% yield). Selected ^{1}H-NMR data δ (acetone-d_6) 7.50 (d, *J* = 8.0 Hz, 1 H), 7.44 (d, *J* = 8.0 Hz, 1 H), 7.33 (d, *J* = 8.0 Hz, 1 H), 7.27–7.14 (m, 10 H), 4.63 (ddd, *J* = 5.1 and 8.2 Hz, 1 H), 4.56 (ddd, *J* = 3.8, 7.8, and 10.0 Hz, 1 H), 4.44–4.40 (m, 1 H), 3.89 (bt, *J* = 6.0 Hz, 1 H), 3.28 (d, *J* = 5.0 Hz, 1 H), 3.11 (dd, *J* = 5.5 and 14.0 Hz, 1 H), 2.95 (d, *J* = 5.0 Hz, 1 H), 2.88 (dd, *J* = 8.2 and 14.2 Hz, 1 H), 2.63–2.57 (m, 2 H), and 1.45 (s 3 H); ESMS (M + H)$^+$ calc'd 592.37, found 593.49.

Purification of 20S proteasome

20S proteasome was purified from bovine reticulocyte lysate by batch DE-52 binding, DEAE-Sephacel chromatography, gel filtration on Sephacryl S-300, and chromatography on hydroxyapatite. This procedure was essentially adopted from a previous procedure [43,44], except that bovine reticulocytes were used as a starting source.

Enzyme kinetic assays

The desired inhibitor and peptide 7-aminomethyl coumarin (AMC) substrate in DMSO (Suc–LLVY–AMC, final assay concentration 5 μM; Z–LLE–AMC, final assay concentration 5 μM; Boc–LRR–AMC, final assay concentration 10 μM) were added to 50 μl assay buffer (20 mM Tris–HCl, pH 8.0, 0.5 mM EDTA; for Suc–LLVY–AMC and Z–LLE–AMC, 0.035% sodium dodecyl sulfate (SDS) was included) and the assay was started by addition of 50 μl assay buffer containing bovine erythrocyte 20S proteasome. The assays were performed at room temperature (22–26°C) in Dyn-Ex Microfluor® 96-well plates and the fluorescence emission was measured at 460 nm (λ_{ex} = 360 nm) using a Cytofluor fluorescence plate reader. Values for $k_{obs}/[I]$ were obtained with the program Kaleidagraph by nonlinear least square fit of the data following the equation for slow and tight binding inhibition [45]: Fluorescence = $_{vst}$ + $[(v_0–v_s)/k_{obs}][1–\exp(–k_{obs}t)]$, were v_0 and v_s are the initial and final velocity respectively, and k_{obs} is the reaction rate constant. The values for $k_{obs}/[I]$ given in Tables 1–4 represent an average of typically nine measurements (generally three independent experiments with three different inhibitor concentrations). Peptide α′,β′-epoxyketones exhibiting low or no inhibition at 150 μM were not tested at higher concentrations in order to avoid problems with low solubility. It is assumed that $k_{obs}/[I]$ values for these compounds are low compared with inhibitors that allow curve-fit to data collected at concentrations lower than 150 μM.

Cell proliferation assays

BAE cells were cultured at 7% CO_2 and were grown in DMEM supplemented with 10% FBS, 1% penicillin/streptomycin (GIBCO), and 1 mM sodium pyruvate. Approximately 1000 cells were plated into each well of a 96-well culture plate. After an overnight incubation, different concentrations of proteasome inhibitors were added and incubation was continued for another 5 days. Subsequently, 74 kBq of [methyl-^{3}H]-thymidine was added to each well and the plate was incubated for an additional 4 h. Cells were harvested using a Skatron Cell Harvester and incorporated radioactivity was quantified using liquid scintillation. Each inhibitor concentration was evaluated in triplicate.

Assay for irritant sensitivity

Irritant sensitivity response assays to DNFB was performed essentially as described previously [46], with slight modifications. In brief, 0-hour ear thickness measurements of both ears were made in triplicate with an engineer's micrometer (Peacock dial thickness gauge, Ozaki Manufacturing Co., LTD., Japan). Five mice per group were subsequently injected intraperiteoneally with epoxomicin (0.32 or 2.0 mg/kg body weight) or with the optimized inhibitor **16** (0.37 or 2.3 mg/kg body weight) in 10% DMSO-phosphate buffered saline. The low dose corresponds to 0.58 μmol/kg and the high dose to 3.6 μmol/kg for both epoxomicin and **16**. The control group of mice received an equal volume of the vehicle (10% DMSO-phosphate buffered saline). After 1 h, mice were challenged on both ear lobes by application of 10 μl of a 0.2% solution of DNFB in acetone:high-grade extra virgin olive oil, 4:1. Ear swelling measurements were made in triplicate 24 h after ear challenge.

Acknowledgements

The authors are grateful to Hak Auth for the preparation of starting materials for the inhibitor syntheses and to David Austin for helpful comments on the manuscript. This work was supported by the NIH (CA-74967). C.M.C. is a Burroughs Wellcome Fund Young Investigator. M.E. was supported by a postdoctoral fellowship from the Swedish Natural Science Research Council, J.M. by an Anderson Fellowship, and U.S. by a fellowship from the Fonds der Chemischen Industrie, Germany.

References

1. Tanaka, K. (1998). Proteasomes: structure and biology. *J. Biochem.* 123, 195-204.
2. Goldberg, A.L., Akopian, T.N., Kisselev, A.F., Lee, D.H. & Rohrwild, M. (1997). New insights into the mechanisms and importance of the proteasome in intracellular protein degradation. *Biol. Chem.* 378, 131-140.
3. King, R.W., Deshaies, R.J., Peters, J.-M. & Kirschner, M.W. (1996). How proteolysis drives the cell cycle. *Science* 274, 1652-1659.
4. Palombella, V.J., Rando, O.J., Goldberg, A.L. & Maniatis, T. (1994). The ubiquitin-proteasome pathway is required for processing the NF-κ B1 precursor protein and the activation of NF-κB. *Cell* 78, 773-785.
5. Tanaka, K. & Kasahara, M. (1998). The MHC class I ligand-generating system: roles of the immunoproteasomes and the interferon-γ-inducible proteasome activator PA28. *Immunol. Rev.* 163, 161-176.
6. Löwe, J., Stock, D., Jap, B., Zwickl, P., Baumeister, W. & Huber, R. (1995). Crystal structure of the 20S proteasome from the archaeon *T. acidophilum* at 3.4 Å resolution. *Science* 268, 533-539.
7. Groll, M., *et al.,* & Huber, R. (1997). Structure of 20S proteasome from yeast at 2.4 Å resolution. *Nature* 386, 463-471.
8. Seemüller, E., Lupas, A., Stock, D., Löwe, J., Huber, R. & Baumeister, W. (1995). Proteasome from *Thermoplasma acidophilum*: a threonine protease. *Science* 268, 579-582.
9. Peters, J.M., Cejka, Z., Harris, J.R., Kleinschmidt, J.A. & Baumeister, W. (1993). Structural features of the 26S proteasome complex. *J. Mol. Biol.* 234, 932-937.
10. Gray, C.W., Slaughter, C.A. & DeMartino, G.N. (1994). PA28 activator protein forms regulatory caps on proteasome stacked rings. *J. Mol. Biol.* 236, 7-15.
11. Orlowski, M., Cardozo, C. & Michaud, C. (1993). Evidence for the presence of five distinct proteolytic components in the pituitary multicatalytic proteinase complex. Properties of two components cleaving bonds on the carboxyl side of branched chain and small neutral amino acids. *Biochemistry* 32, 1563-1572.
12. Lee, D.H. & Goldberg, A.L. (1998). Proteasome inhibitors: valuable new tools for cell biologists. *Trends Cell Biol.* 8, 397-403.
13. Rolfe, M., Chiu, M.I. & Pagano, M. (1997). The ubiquitin-mediated proteolytic pathway as a therapeutic area. *J. Mol. Med.* 75, 5-17.
14. Spataro, V., Norbury, C. & Harris, A.L. (1998). The ubiquitin-proteasome pathway in cancer. *Br. J. Cancer* 77, 448-455.
15. Fenteany, G., Standaert, R.F., Lane, W.S., Choi, S., Corey, E.J. & Schreiber, S.L. (1995). Inhibition of proteasome activities and subunit-specific amino-terminal threonine modification by lactacystin. *Science* 268, 726-731.
16. Adams, J., *et al.,* & Stein, R.L. (1998). Potent and selective inhibitors of the proteasome: dipeptidyl boronic acids. *Bioorg. Med. Chem. Lett.* 8, 333-338.
17. Rock, K.L., *et al.,* & Goldberg, A.L. (1994). Inhibitors of the proteasome block the degradation of most cell proteins and the generation of peptides presented on MHC class I molecules. *Cell* 78, 761-771.
18. McCormack, T., *et al.,* & Dick, L. (1997). Active site-directed inhibitors of Rhodococcus 20S proteasome. Kinetics and mechanism. *J. Biol. Chem.* 272, 26103-26109.
19. Figueiredo-Pereira, M.E., Berg, K.A. & Wilk, S. (1994). A new inhibitor of the chymotrypsin-like activity of the multicatalytic proteinase complex (20S proteasome) induces accumulation of ubiquitin-protein conjugates in a neuronal cell. *J. Neurochem.* 63, 1578-1581.
20. Spaltenstein, A., *et al.,* & Crouch, R. (1996). Design and synthesis of novel protease inhibitors. Tripeptide α′,β′-epoxyketones as nanomolar inactivators of the proteasome. *Tetrahedron Lett.* 37, 1343-1346.
21. Sin, N., Kim, K., Elofsson, M., Meng, L., Auth, H. & Crews, C.M. (1999). Total synthesis of the potent proteasome inhibitor epoxomicin: a useful tool for understanding proteasome biology. *Bioorg. Med. Chem. Lett.* 9, 2283-2288.
22. Meng, L., Mohan, R., Kwok, B.H.B., Elofsson, M., Sin, N. & Crews, C.M. (1999). Epoxomicin, a potent and selective proteasome inhibitor, exhibits *in vivo* anti-inflammatory activity. *Proc. Natl Acad. Sci. USA* 96, 10403-10408.
23. Meng, L., Kwok, B.H.B., Sin, N. & Crews, C.M. (1999). Eponemycin exerts its antitumor effect through inhibition of proteasome function. *Cancer Res.* 59, 2798-2801.
24. Lynas, J.F., Harriott, P., Healy, A., McKervey, M.A. & Walker, B. (1998). Inhibitors of the chymotrypsin-like activity of proteasome based on di- and tri-peptidyl α-keto aldehydes (glyoxals). *Bioorg. Med. Chem. Lett.* 8, 373-378.
25. Bogyo, M., Shin, S., McMaster, J.S. & Ploegh, H.L. (1998). Substrate binding and sequence preference of the proteasome revealed by active-site-directed affinity probes. *Chem. Biol.* 5, 307-320.
26. Bogyo, M., McMaster, J.S., Gaczynska, M., Tortorella, D., Goldberg, A.L. & Ploegh, H. (1997). Covalent modification of the active site threonine of proteasomal β subunits and the *Escherichia coli* homolog HslV by a new class of inhibitors. *Proc. Natl Acad. Sci. USA* 94, 6629-6634.
27. Palmer, J.T., Rasnick, D., Klaus, J.L. & Brömme, D. (1995). Vinyl sulfones as mechanism-based cysteine protease inhibitors. *J. Med. Chem.* 38, 3193-3196.
28. Ostrowska, H., Wojcik, C., Omura, S. & Worowski, K. (1997). Lactacystin, a specific inhibitor of the proteasome, inhibits human platelet lysosomal cathepsin A-like enzyme. *Biochem. Biophys. Res. Commun.* 234, 729-732.
29. Geier, E., *et al.,* & Niedermann, G. (1999). A giant protease with potential to substitute for some functions of the proteasome. *Science* 283, 978-981.
30. Craiu, A., *et al.,* & Rock, K.L. (1997). Lactacystin and clasto-lactacystin beta-lactone modify multiple proteasome β-subunits and inhibit intracellular protein degradation and major histocompatibility complex class I antigen presentation. *J. Biol. Chem.* 272, 13437-13445.
31. Loidl, G., Groll, M., Musiol, H.-J., Huber, R. & Moroder, L. (1999). Bivalency as a principle for proteasome inhibition. *Proc. Natl Acad. Sci. USA* 96, 5418-5422.
32. Loidl, G., Groll, M., Musiol, H.-J., Ditzel, L., Huber, R. & Moroder, L. (1999). Bifunctional inhibitors of the trypsin-like activity of eukaryotic proteasomes. *Chem. Biol.* 6, 197-204.
33. Hanada, M., *et al.* & Oki, T. (1992). Epoxomicin, a new antitumor agent of microbial origin. *J. Antibiotics* 45, 1746-1752.
34. Sugawara, K., *et al.* & Oki, T. (1990). Eponemycin, a new antibiotic active against B16 melanoma. I. Production, isolation, structure and biological activity. *J. Antibiotics* 43, 8-18.
35. Sin, N., Meng, L., Auth, H. & Crews, C.M. (1998). Eponemycin analogs: synthesis and use as probes of angiogenesis. *Bioorg. Med. Chem.* 6, 1209-1217.
36. Crews, C.M. & Splittgerber, U. (1999). Chemical genetics: exploring and controlling cellular processes with chemical probes. *Trends Biochem. Sci.* 24, 317-320.
37. Fields, G.B. & Noble, R.L. (1990). Solid phase peptide synthesis utilizing 9-fluorenylmethoxycarbonyl amino acids. *Int. J. Pept. Protein Res.* 35, 161-214.
38. Grant, G.A. (1992). Synthetic peptides. In *A User's Guide*. (Grant, GA, ed.) W.H. Freeman and Company, New York, USA.
39. Carpino, L.A. (1993). 1-Hydroxy-7-azabenzotriazole. An efficient peptide coupling additive. *J. Am. Chem. Soc.* 115, 4397-4398.
40. Carpino, L.A., El-Faham, A. & Albericio, F. (1994). Racemization studies during solid-phase peptide synthesis using azabenzotriazole-based coupling reagents. *Tetrahedron Lett.* 35, 2279-2282.
41. Roush, W.R., Gonzalez, F.V., McKerrow, J.H. & Hansell, E. (1999). Design and synthesis of dipeptidyl α′, β′-epoxyketones, potent and irreversible inhibitors of the cysteine protease cruzain. *Bioorg. Med. Chem. Lett.* 8, 2809-2812.
42. Grabbe, S., Steinert, M., Mahnke, K., Schwartz, A., Luger, T.A. & Schwarz, T. (1996). Dissection of antigenic and irritative effects of epicutaneously applied haptens in mice. Evidence that not the antigenic component but nonspecific proinflammatory effects of haptens determine the concentration-dependent elicitation of allergic contact dermatitis. *J. Clin. Invest.* 98, 1158-1164.
43. McGuire, M.J. & DeMartino, G.N. (1986). Purification and characterization of a high molecular weight proteinase (macropain) from human erythrocytes. *Biochim. Biophys. Acta* 873, 279-289.
44. McGuire, M.J., McCullough, M.L., Croall, D.E., & DeMartino, G.N. (1989). The high molecular weight multicatalytic proteinase, macropain, exists in a latent form in human erythrocytes. *Biochim. Biophys. Acta* 995, 181-186.
45. Morrison, J.F. & Walsh, C.T. (1988). The behavior and significance of slow-binding enzyme inhibitors. *Adv. Enzymol. Relat. Areas Mol. Biol.* 61, 201-301.
46. Kehren, J., *et al.,* & Nicolas, J.F. (1999). Cytotoxicity is mandatory for CD8(+) T cell-mediated contact hypersensitivity. *J. Exp. Med.* 189, 779-786.

Because *Chemistry & Biology* operates a 'Continuous Publication System' for Research Papers, this paper has been published via the internet before being printed. The paper can be accessed from http://biomednet.com/cbiology/cmb – for further information, see the explanation on the contents pages.